

## A Study of SST Warming Trend in the Western Equatorial Pacific in a Coupled Ocean–Atmosphere–Land GCM<sup>①</sup>

Liu Hui (刘 辉) and Zhang Xuehong (张学洪)

*State Key Laboratory of Numerical Modeling for Atmospheric Sciences and Geophysical Fluid Dynamics (LASG).*

*Institute of Atmospheric Physics, Chinese Academy of Sciences*

*P. O. Box 2718, Beijing 100080*

(Received January 22, 1998; revised July 28, 1998)

### ABSTRACT

In a version of LASG coupled ocean–atmosphere–land system model, where a diurnal cycle of solar radiation is included, a rapid SST warming trend of about 2.0°C appears in the western equatorial Pacific within the first two years of an integration. An analysis reveals that the appearance of the surface westerly wind anomaly since the fifth month of the integration is responsible for the SST warming. To reduce the SST warming, the reference heat flux used in the model is then redefined according to the first 4 months, instead of the first 3 years, of a trial run. It is found that the refining of the reference heat flux is successful in avoiding the unrealistic persistent westerly wind anomaly. Consequently, the SST warming is almost completely removed. It is explored that the persistent westerly wind anomaly is induced by the anomalous surface pressure patterns in the northern tropical and subtropical regions, which is related to the errors in the surface heat flux in the off-equatorial regions.

**Key words:** Ocean–atmosphere–land, System model, Western equatorial Pacific, Flux anomaly

### 1. Background

A global ocean–atmosphere–land system general circulation model (GCM) has been developed in the State Laboratory of Numerical Modeling for Atmospheric Sciences and Geophysical Fluid Dynamics (LASG) since 1994, which is composed of a nine-layer R15 AGCM and a twenty-layer  $4^\circ \times 5^\circ$  global OGCM with a simple biosphere model included (see Wu et al., 1997 for Version 1 of the model). The ocean and atmosphere model are coupled with the monthly flux anomalies (MFA) of heat and momentum to reduce the impact of systematic errors of each component model on the coupled system. The flux anomaly is defined as  $\delta F = F^C - F_0^R$ , where  $F^C$  is the flux computed simply by the coupled model itself, and  $F_0^R$  is a reference flux taken from the uncoupled climatology (Zhang et al., 1992) and may be referred to as “zero-order” reference flux. The earliest version (Version 0) of the model coupled in this way, however, still suffered evident warming trend reflecting the global mean SST increases about 1.0 K during the first several years (Liu et al., 1996).

To reduce the trend in the global mean SST, a modified MFA scheme (MMFA) is proposed by Yu et al. (1997). In MMFA,  $F_0^R$  is replaced by a “first-order” reference flux,

<sup>①</sup>This work was supported by CNSF projects No. 49475255, 49575265, and National key project studies on short-range climate prediction system in China (No. 96-908-04-03-3 and 96-908-02-03-4).

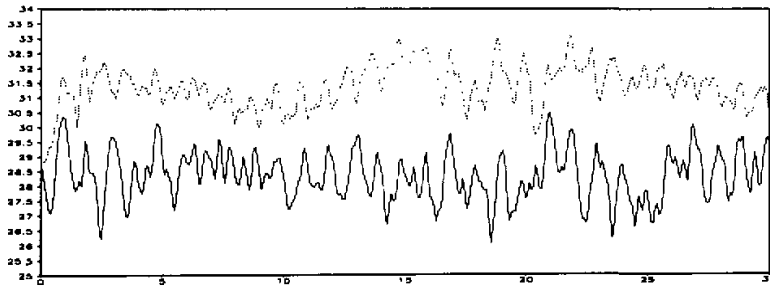


Fig. 1. Time evolution of monthly SST averaged over the region of 157.5–172.5°E, 4°N–4°S for two 30-year integrations of the coupled model (dashed line is for MMFA( $Y=3$ ) and solid line for MMFA( $M=4$ )), unit: K.

$F_1^R = F_0^R + \overline{\delta F}$ , where  $\overline{\delta F} = \frac{1}{Y} \sum_{j=1}^Y (F^C - F_0^R)$  is the flux anomaly averaged over the first

$Y$  years of a trial run of the coupled model with the MFA scheme which is based on the “zero-order” reference flux. It should be noted that  $\delta F$  here represents a multi-year averaged *monthly mean* correction to  $F_0^R$  and  $Y$  is special for indicating the total number of years for the averaging. The choice of  $Y$  is somewhat arbitrary. In several experiments before this study,  $Y$  is set to 3, and it is found that the MMFA with  $Y=3$  can effectively reduce the warming trend in the global mean SST. In short, the coupling scheme used in those experiments can be referred to as “MMFA( $Y=3$ )”.

Although the warming trend of the global mean SST, which is mainly governed by the global mean surface heat flux, is small enough to be ignored with this improved coupling scheme, the temporal behavior of the regionally averaged SST, which is affected by not only the surface heat flux but also the ocean dynamics, may not be satisfactory everywhere. This is indeed the case in Version 3 of the model, where a diurnal variation of solar radiation is included. The dashed line shown in Fig. 1 is the 30-year temporal evolution of the SST anomaly averaged over a region in the western equatorial Pacific, that is, 157.5–172.5°E, 4°N–4°S. The regional mean SST increases about two degrees after integration of only two years. After that, it reaches a new equilibrium state which is apparently warmer than the initial one. The results show that the coupling scheme MMFA( $Y=3$ ), which is successful in controlling the drift of the global mean SST, may not be able to overcome some evident trends of SST in some specific areas.

In this paper, the possible causes for the regional warming of SST are explored and some refinements of the MMFA are designed to reduce the warming. On the basis of successful performance of the refined MMFA, the influence of the air–sea interaction in some off-equatorial areas on the SST behavior in the western equatorial Pacific is discussed.

## 2. Analysis of the regional SST warming

To explore the SST warming, a trial run of Version 3 of the model with MFA is performed first. Fig. 2 shows the time evolution of the anomalies of zonal wind stress, SST, and

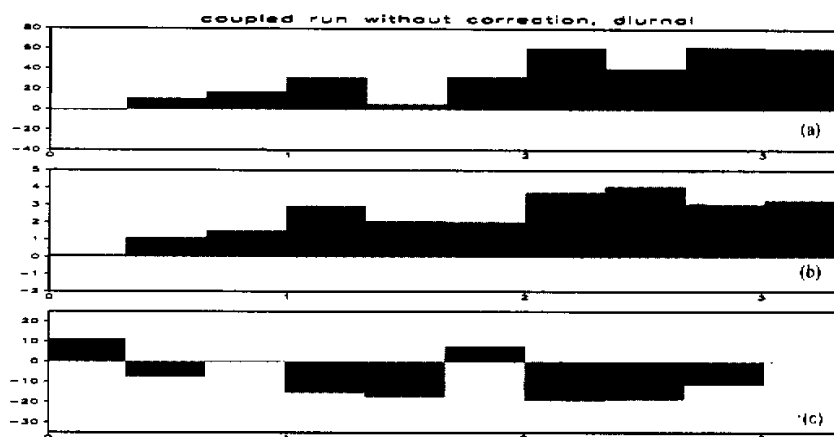


Fig. 2. Time evolution of the anomalies averaged over the region of  $157.5^{\circ}\text{E}$ – $172.5^{\circ}\text{E}$ ,  $4^{\circ}\text{N}$ – $4^{\circ}\text{S}$  of zonal wind stress (a), SST (b), and heat flux (c) for a trial run with MFA. Heat flux into ocean is defined as positive. Units for wind stress and heat flux are:  $10^{-3} \text{ N m}^{-2}$  and  $\text{W m}^{-2}$  respectively.

heat flux for the first three years of the trial run. The anomalies are averaged over a specific area in the western equatorial Pacific, i.e., the region of  $157.5^{\circ}\text{E}$ – $172.5^{\circ}\text{E}$ ,  $4^{\circ}\text{N}$ – $4^{\circ}\text{S}$ . In this figure, the anomalies are averaged for every 4 months consecutively. For example, the value in the first column is the average from January to April and the second from May to August, etc.. It can be seen from Fig. 2(a) that the zonal wind stress anomaly appears a weak easterly during the first four months and then becomes a very strong westerly in the following almost whole period. The magnitude of the persistent westerly anomaly can reach about  $60 \times 10^{-3} \text{ N m}^{-2}$  from the third year onward, much stronger than that of the observed wind stress in this region where the trades reach its western end.

Corresponding to the anomalous westerly, significant positive SST anomaly can be found from the second episode of four months: more than two degrees during the second year and 3 degrees during the third year (see Fig. 2(b)). In the heat flux anomaly shown in Fig. 2(c), there is an evident transfer from strong downward in the first four months to dominantly upward afterwards. It is quite clear that the persistent westerly wind stress anomaly is the major cause for the SST warming during the whole period and the heat flux anomaly is just a consequence of the SST warming.

Thus, the question is how to avoid the appearance of the persistent westerly anomaly since the second 4 months. The wind anomaly should result from some kind of anomalous atmospheric pressure patterns, which may be, in turn, related to the anomalous surface heat flux. Consequently, the appearance of the wind anomaly should result from errors in heat flux. Although the local heat flux anomaly in the specific region mentioned above seems not to be the direct cause for the westerly anomaly, it must be an indicator for errors in heat flux in remote regions. Moreover, considering significant signals of the warming trend and associated westerly anomaly appear since the second 4 months, we should pay much attention to the heat flux errors during the first four months. To test this idea, an experimental run is done with the reference heat flux defined by the first 4-month data rather than multi-year data, i.e.

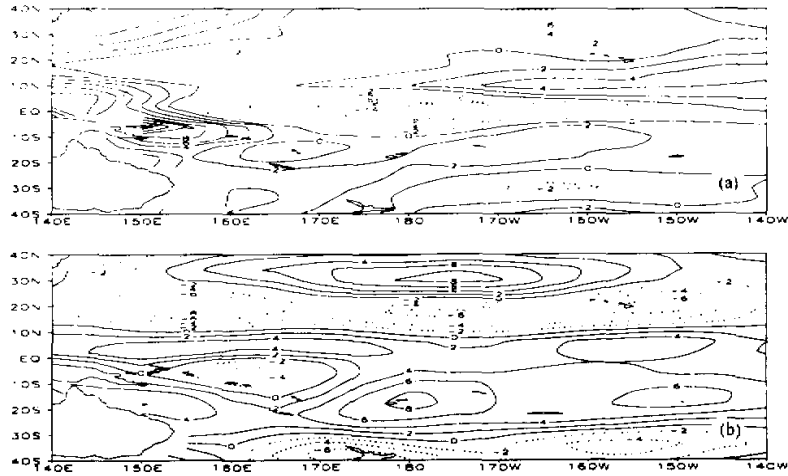


Fig. 3.  $\overline{\delta F}$  averaged over the first three years (a) and over the first 4 months (b) of a trial run with MMFA, unit:  $\text{W m}^{-2}$ .

$\overline{\delta F} = \frac{1}{M} \sum_{m=1}^M (F^C - F_0^R)$  and  $M = 4$ . Different from that used in the previous experiments,  $\overline{\delta F}$  here represents a multi-month averaged *time-independent* correction to the reference flux, and  $M$  is special for indicating the total number of months for the averaging. The corresponding coupling scheme can be referred to as MMFA( $M=4$ ) which is formally similar to MMFA( $Y=3$ ). It should be kept in mind, however, that the former uses an  $M$ -month averaged *time-independent*  $\overline{\delta F}$  and the latter uses a  $Y$ -year averaged  $\overline{\delta F}$  with seasonal cycle. An integration of 30 years with MMFA( $M=4$ ) is done and it is referred to Run I. Some results of Run I will be discussed in the following sections.

Figs. 3(a) and (b) show respectively  $\overline{\delta F}$  used in MMFA( $Y=3$ ) and that used in MMFA( $M=4$ ) in a part of the Pacific Ocean. There are dramatic differences between them in the equatorial Pacific region where the former is negative in most of the longitudes and the latter is positive almost everywhere. There are also large differences in some off-equatorial areas especially in the northern tropical and subtropical regions. For example, in the zone around 20°N,  $\overline{\delta F}$  is positive in the eastern and negative in the western part of the basin for the case of MMFA( $Y=3$ ) (Fig. 3(a)), but negative everywhere for the case of MMFA( $M=4$ ) (Fig. 3(b)). The reversed patterns of  $\overline{\delta F}$  can be found in the zone around 30°N in the cases of both MMFA( $Y=3$ ) and MMFA( $M=4$ ). As it will be seen later, it is the differences in the off-equatorial region of the two  $\overline{\delta F}$ 's that result in the different wind stress patterns: The persistent westerly anomaly occurs in the run with MMFA( $Y=3$ ) but not in Run I with MMFA( $M=4$ ).

### 3. Improvement due to refining MMFA

The time evolution of the anomaly of zonal wind stress for the first 3 years of Run I is presented in Fig. 4(a). In comparison with Fig. 2(a), the westerly anomaly is greatly reduced

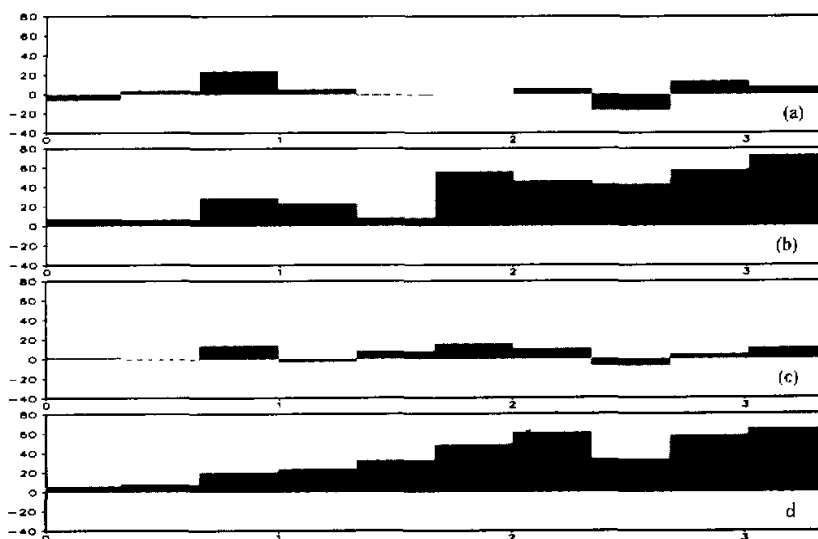


Fig. 4. Time evolution of zonal wind stress anomaly averaged over the region of 157.5–172.5°E, 4°N–4°S for model runs with MMFA( $M=4$ ) (a), MMFA( $Y=3$ ) (b), MFA, but only coupled with-in 8°N–8°S (c), and MMFA( $M=4$ ), but used only within 8°N–8°S (d), unit:  $10^{-3} \text{ N m}^{-2}$ .

with its maximum less than  $20 \times 10^{-3} \text{ N/m}^2$  and an easterly anomaly of about  $-20 \times 10^{-3} \text{ N/m}^2$  even appears in the eighth period of four months. As a result, there is no persistent westerly anomaly during the whole period. Instead, the interannual variability of wind stress becomes more significant. As a contrast, Fig. 4(b) shows the zonal wind stress anomaly given by running Version 3 with MMFA( $Y=3$ ). The contrast becomes quite sharp starting from the second year: a strong and persistent westerly anomaly, which disappears from Fig. 4(a), can still be found in Fig. 4(b). Another experimental run with MMFA( $Y=1$ ) does not show any essential improvements in comparison with the results given by MMFA( $Y=3$ ). This strongly suggests that selection of time period for calculating  $\delta F$  has important impact on the ability of coupling scheme MMFA in controlling regional climate drift at least in the equatorial western Pacific region. For Version 3 of the model, MMFA( $M=4$ ) seems to be a better choice than MMFA( $Y=3$ ) or MMFA( $Y=1$ ).

The time evolution of the monthly SST averaged over the specific region for the whole 30 years of Run I is shown in Fig. 1 by solid line. It can be seen that there is no evident warming of SST during the period. The mean value of SST during the 30-year integration is about 29°C, much closer to the observed mean value of COADS data for the period of 1960–1989 (not shown here).

#### 4. Off-equatorial impact on the regional SST behavior

The analyses in the previous sections have revealed that the SST anomalies in the western equatorial Pacific region are mainly driven by the local wind stress anomaly rather than the surface heat flux anomaly. In general, the wind stress anomaly is strongly related to the anomalous surface pressure which may have direct interaction with the SST anomaly through

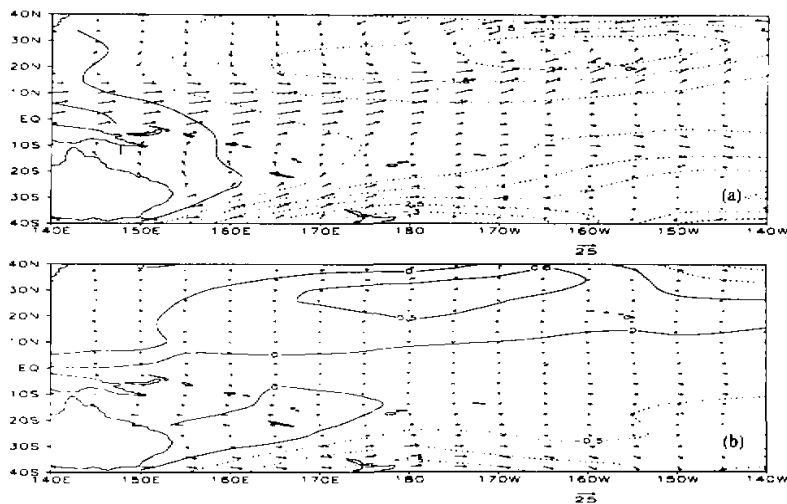


Fig. 5. Surface pressure and wind stress anomalies averaged over the first 3 years of the trial run (a) and Run I (b), unit for pressure: hPa, contour interval: 0.5 hPa. The maximum vector for wind stress represents  $25 \times 10^{-3} \text{ N m}^{-2}$ .

the air-sea heat exchange. Therefore, investigating changes of pressure may be helpful to explore how the westerly anomaly is produced. Figs. 5(a) and (b) show the surface pressure anomaly and the corresponding anomalous wind stress vector averaged for the first 3 years of Run I and the trial run with MFA respectively. It can be seen from Fig. 5(a) that there exists a large-scale negative surface pressure anomaly with its central value of about 2.5 hPa near  $165^\circ\text{W}$ ,  $25^\circ\text{N}$  and a weak positive pressure anomaly over New Guinea and the northern Australia. In association with this surface pressure pattern, a strong ageostrophic wind blows from the positive pressure anomaly to the negative one in the northern tropical and subtropical regions, resulting in the dramatic anomalous westerly component of wind stress in the western equatorial Pacific area. Obviously, the pressure pattern especially the existence of the negative pressure anomaly in the northern subtropics is responsible for the occurring of the persistent westerly anomaly in the equatorial western Pacific.

In Run I, the surface pressure anomaly (Fig. 5(b)) is much weaker in comparison with that of the trial run. As shown in Fig. 5(b), the pressure anomaly in equatorial western Pacific is almost zero. Meanwhile, in the northern off-equatorial regions, there is a weak positive pressure anomaly of 0.5 hPa centered at about  $175^\circ\text{W}$ ,  $25^\circ\text{N}$ . As a result, the wind stress anomaly is very weak almost everywhere especially in the equatorial western Pacific region. In this case, the westerly anomaly and the associated heat flux anomaly in the western equatorial Pacific region seems to be closely related to the pattern of anomalous surface pressure mainly in the northern subtropical high region.

To make this more clear, an experimental run is done, where the AGCM and OGCM components are coupled only within an equatorial belt ( $8^\circ\text{S}$ – $8^\circ\text{N}$ ) and other aspects of the model are identical with the trial run using MFA. In other words, the possible impact of the heat flux errors from the off-equatorial regions on the SST anomaly in the equatorial region is totally cut off in this experiment. The zonal wind stress anomaly averaged in the equatorial

western Pacific area is shown in Fig. 4(c). It can be seen that the wind stress anomaly becomes very weak and is quite similar to that in Fig. 4(a). It is obvious that the persistent westerly anomalies in the western equatorial Pacific cannot be triggered without the air-sea coupling in some off-equatorial regions.

The above finding has been further confirmed by another experiment where  $\overline{\delta F}$  with MMFA ( $M=4$ ) is adapted only in the region of  $8^{\circ}\text{S}$ – $8^{\circ}\text{N}$ . This experiment enables us to see whether or not correcting the errors of heat flux only in the equatorial region can reduce the westerly anomaly. As it is expected that a persistent and strong westerly anomaly still exists during the period of this experiment (see Fig. 4(d)). It means that refining the local  $\overline{\delta F}$  only in the equatorial region has no positive contribution to reducing the persistent westerly anomaly.

## 5. Summary

Possible causes for the strong SST warming trend in the western equatorial Pacific in the coupled ocean-atmosphere-land system model GCM of LASG are investigated in this paper. It is shown that the SST warming results from the persistent westerly stress anomaly. It is explored that the westerly anomaly mainly comes from the errors of heat flux in some off-equatorial regions. A reference heat flux defined from the first 4 months, instead of the first 3 years, of a trial run is able to effectively avoid the occurring of the persistent westerly stress anomaly. With this refined reference flux, the simulation of SST is apparently improved in this region.

## REFERENCES

- Liu, H., X. Z. Jin, X. H. Zhang, and G. X. Wu, 1996: A coupling experiment of an atmosphere and an ocean model with a monthly anomaly exchange scheme. *Adv. Atmos. Sci.*, **13**(2), 133–146.
- Liu, H., X. H. Zhang, and G. X. Wu, 1998: Cloud feedback on SST variability in the western equatorial Pacific in GOALS/LASG model. *Adv. Atmos. Sci.*, **15**(3), 411–423.
- Yu, Y. Q., and X. H. Zhang, 1997: A modified air-sea flux anomaly coupling scheme. *Chinese Science Bulletin*, **43**(8), 866–870 (in Chinese).
- Wu, G. X., H. Liu, Y. C. Zhao, and W. P. Li, 1996: A nine-layer atmospheric general circulation model and its performance. *Adv. Atmos. Sci.*, **13**(1), 1–18.
- Wu, G. X., X. H. Zhang, H. Liu et al., 1997: Global ocean-atmosphere-land system model of LASG (GOALS/LASG) and its performance in simulation study. *Quarterly Journal of Applied Meteorology*, **8**(Suppl.), 15–28 (in Chinese).
- Zhang X. H., N. Bao, R. C. Yu, and W. Q. Wang, 1992: Coupling experiments based on an atmospheric and an oceanic GCM. *Chinese Journal of Atmospheric Sciences*, **16**, 129–144.
- Zhang X. H., K. M. Chen, X. Z. Jin, W. Y. Lin, and Y. Q. Yu, 1996: Simulation of thermohaline circulation with a twenty-layer oceanic general circulation model. *Theoretical and Applied Climatology*, **55**, No. 1–4, 65–88.